Supplementary Information

Boosting the Crystallinity of Novel Two-Dimensional Hexamine Dipyrazino Quinoxaline-Based Covalent Organic Framework for Electrical Double-Layer Supercapacitor

Rashid Iqbal[a,b,c]*, Muhammad Kashif Majeed[d], Arshad Hussain[b,c], Aziz Ahmad[e], Muhammad Ahmad[b,c], Bushra Jabbar[c,h], Abdul Rehman Akbar[b,c], Sajjad Ali[f], Sajid Rauf[g], Adil Saleem[c,h]*

[a]*Key Laboratory of Colloid and Interface Chemistry of the Ministry of Education, School of Chemistry and Chemical Engineering, Shandong University, 250100 Jinan, China.*

[b]*Institute for Advanced Study, Shenzhen University, Shenzhen 518060, China.*

[c]*College of Physics and Optoelectronic Engineering, Shenzhen University, Shenzhen 518060, China.*

[d]*Materials Chemistry Laboratory, Department of Materials Science & Engineering, The University of Texas at Arlington, Arlington, TX, USA.*

[e]*Interdisciplinary Research Center for Hydrogen and Energy Storage (IRC-HES), King Fahd University of Petroleum & Minerals, KFUPM Box 5040, Dhahran 31261, Saudi Arabia.*

[f]*Yangtze Delta Region Institute (Huzhou), University of Electronic Science and Technology of China, Huzhou, 313001, China.*

[g]*College of Electronics and Information Engineering, Shenzhen University, Guangdong Province 518000, China.*

[h]*College of Mechatronics and Control Engineering, Shenzhen University, Shenzhen, Guangdong 518060, China.*

Catalogue

Section 1. Materials and Methods

The reported approach was used to create 2,3,6,7,10,11-hexaamine dipyrazino quinoxaline. [1] Hexane, ethyl acetate, sodium terbutoxide, benzophenone imine, tetrahydrofuran, cobalt chloride hexahydrate, acetic acid, concentrated nitric acid, iron powder, and diethyl ether are among the chemicals used in this process. The following substances were bought from Sigma Aldrich: 1, 2-dichlorobenzene, nitro benzene, bromine water, tris(dibenzylideneacetone)dipalladium (0), dichlorometane, silica gel, ethyl acetate, n-hexane, deuterated chloroform, and deuterated dimethyl sulfoxide. A JASCO model FT IR-6100 Fourier transform infrared spectrometer was used to record infrared (IR) spectra. Field ionization On a Hitachi model S-4200, scanning electron microscopy (FESEM) was carried out. FE-SEM running at 5.0 kV of accelerating voltage. On a Tecnai model F-20 microscope, transmission electron microscopy (TEM) images were captured. On a Rigaku RINT

Ultima III diffractometer, data from powder x-ray diffraction (PXRD) were collected. On a Shimadzu DT-30B, thermo gravimetric analysis (TGA) measurements were made with a continuous N2 purge and a heating rate of 5 °C/min from ambient temperature to 1000 °C. Using an ASAP 2020, the samples' nitrogen sorption/desorption isotherms were measured at 77.15K. (Micromeritics). The materials were outgassed prior to adsorption for six hours at 150 °C and 10-6 Torr of vacuum. The specific surface area and pore size distribution were calculated, respectively, using the Brunauer-Emmett-Teller (BET) technique and the density functional theory (DFT) pore model. At a base pressure of 110^{-9} mbar and using an Al K X-ray source, an ESCALAB250 apparatus was used to conduct the X-ray photoelectron spectroscopy (XPS) measurement.

1.2. XRD Pawley Refinement

Reflex in MS modeling ver. 6.0 was used to refine the Pawley model (Accelrys Inc.). First, using the hexagonal crystal structure, we manually determined the unit cell's size from the observed experimental XRD peak positions. With the aid of the computed dimensions of the unit cell, the lattice parameters were refined using the Pawley method until the RWP value converged. The findings reveal a hexagonal crystal system with unit cell parameters of α=β=90° and gamma=120°, together with a=b=15.650 A° and c=3.49006 A°. The pseudo-Voigt and Berrar-Baldinozzi functions were used for profile fitting and asymmetry correction. 2.73 percent and 1.23 percent, respectively, were the final RWP and RP figures.

1.3. Electrochemical Measurements

With $EMIMBF_4$ and 1M H_2SO_4 acting as the appropriate electrolytes, electrochemical tests were carried out in a conventional two-electrode symmetric supercapacitor system (a coin-type cell of 2032 size). The HADQ COF (85 weight percent, around 100 mg), carbon black (10 weight percent, Super P conductive), and polytetrafluoroethylene (5 weight percent, 60 percent in water, and diluted to 6 percent before use) were typically ground in an agate mortar to create the electrode films. The

electrode film was cut into a circle with a 12 mm diameter and a mass of around 0.7–1 mg after being vacuum-dried at 120 °C for 12 hours. Two electrodes with nearly the same mass were pressed in between stainless-steel wire meshes (316L, 400 meshes, the diameter of 15 mm) respectively as the two symmetric working electrodes. A coin-type cell was constructed using Glass fiber film (Whatman) as a separator, which was subsequently bathed in $EMIMBF_4$ and 1M H_2SO_4 electrolyte. On a CHI660D electrochemical workstation set up at room temperature, CV curves, galvanostatic charge–discharge curves, and Nyquist plots were gathered. The formula C = 2It/(mV), where I (unit: A) is the discharge current, m (unit: g) is the mass of HADQ COF in one electrode, t (unit: s) is the discharge time, and V (unit: V) is the discharge voltage, was used to determine the specific capacitance (C, F/g) from the slop of the discharge curve. $E = (1000*CV^2)/(8/3600)$ was used to calculate the energy densities (E, Wh/kg). P = E/(t/3600) was used to compute the power densities (P, W/kg).

Section 2. Elemental composition of pristine HADQ COF, 200-HADQ COF and 250-HADQ COF

Table S1. Elemental composition of HADQ COF from different characterization techniques.

Technique	C	H	N	O	Total
Theoretical (wt.%)	**51.44**	**0.96**	**39.99**	**7.61**	**100**
EA (wt.%)[a]	**48.63**	**3.64**	**39.45**	**8.26**	**99.98**
XPS (at.%)[b]	**61.4**	**N. A**	**32.4**	**6.2**	**100**

200-HADQ COF

Technique	C	H	N	O	Total
Theoretical (wt.%)	60.00	1.12	38.88	0	100
EA (wt.%)[a]	58.01	1.91	37.32	2.72	99.96
XPS (at.%)[b]	**68.3**	**N. A**	**29.6**	**2.1**	**100**

250-HADQ COF

Technique	C	H	N	O	Total
EA (wt.%)[a]	61.21	1.08	36.45	1.24	99.98

[a] EA is most reliable element counts for bulk sample. The higher oxygen and hydrogen contents than theoretical calculation should be due to trapped small molecules (moisture, oxygen, and etc.) in the holes and interlayers of the HADQ COF.

[b] XPS is more sensitive to surface chemical composition.

Section 3. XPS spectroscopies of pristine HADQ COF, 200-HADQ COF and 250-HADQ COF

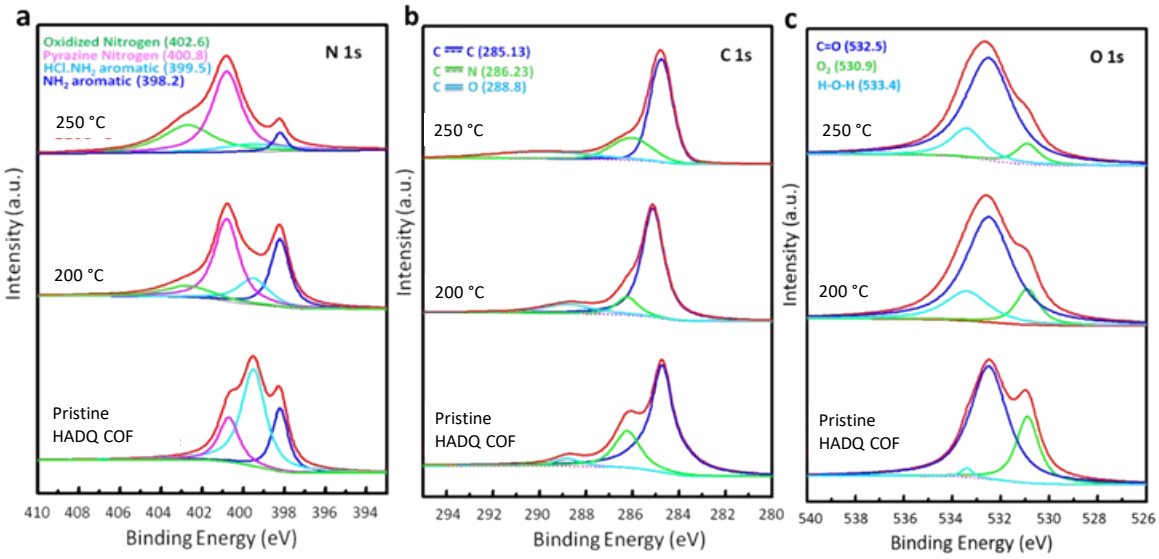

Figure S1. XPS Spectra of pristine HADQ COF, 200-HADQ COF and 250-HADQ COF: (a) C 1s. (b) N 1s. (c) O 1s.

Section 4. FE SEM Images of HADQ COF

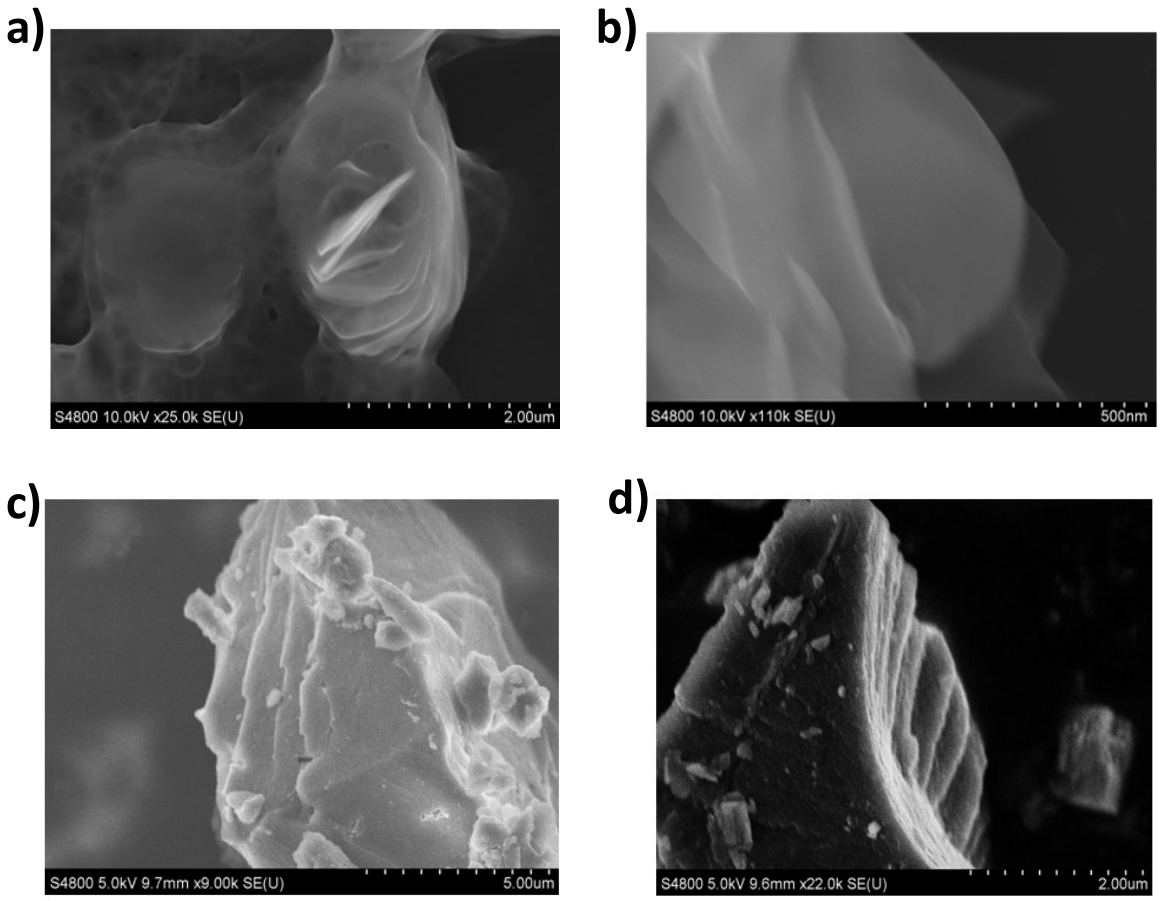

Figure S2. (a-b) SEM images of 250-HADQ COF and pristine HADQ COF.

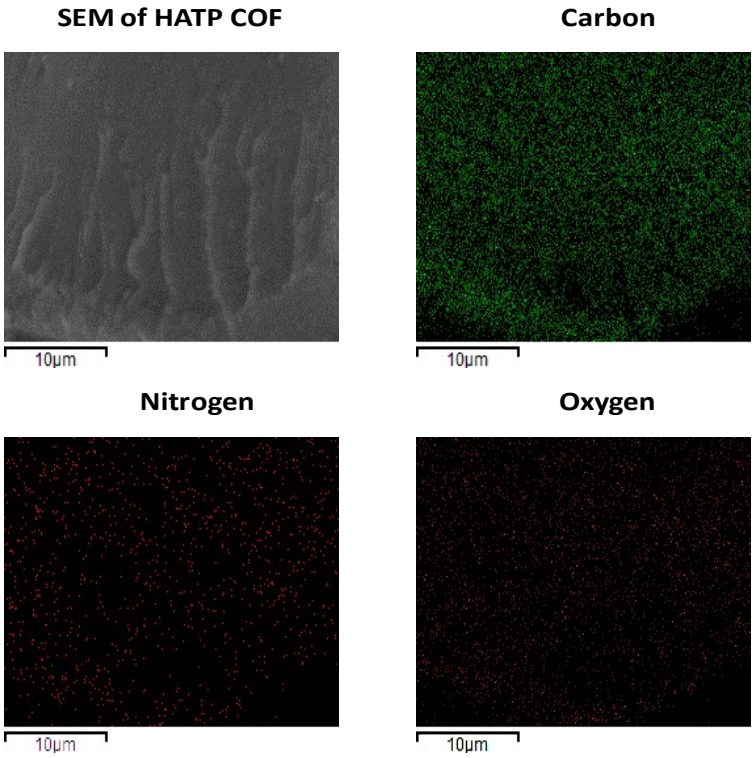

Figure S3. SEM mapping of 250-HADQ COF, Carbon mapping, Nitrogen mapping, Oxygen mapping.

Section 5. Surface Parameters of pristine HADQ COF, 200-HADQ COF and 250-HADQ COF

Table S2. Surface parameters of pristine HADQ COF, 200-HADQ COF and 250-HADQ COF.

	Pristine HADQ COF	200 °C	250 °C
BET Surface Area (m^2/g)	746	1453	2977
Pore Volume (cm^3/g)	0.98	1.09	1.25

Section 6. EIS Profiles of 250-HADQ COF in $EMIMBF_4$ and 1 M H_2SO_4

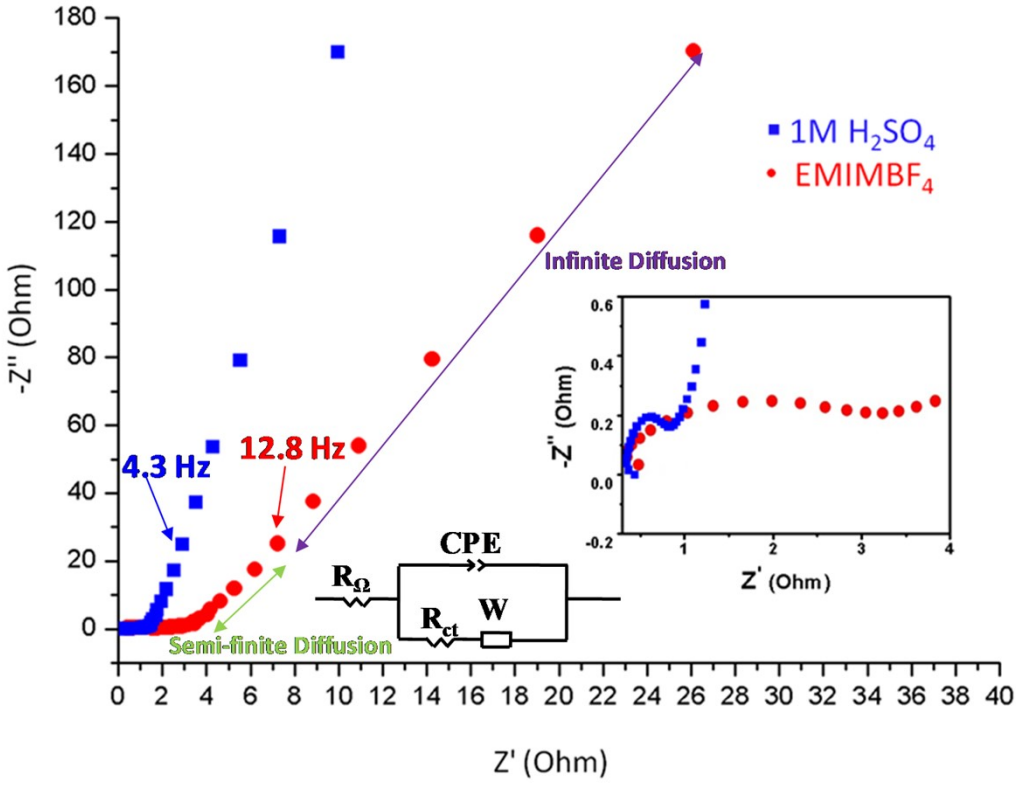

Figure S4. EIS Profiles of 250-HADQ COF in $EMIMBF_4$ and 1 M H_2SO_4.

Section 7. Electrochemical performance measured in and $EMIMBF_4$ and 1 M H_2SO_4

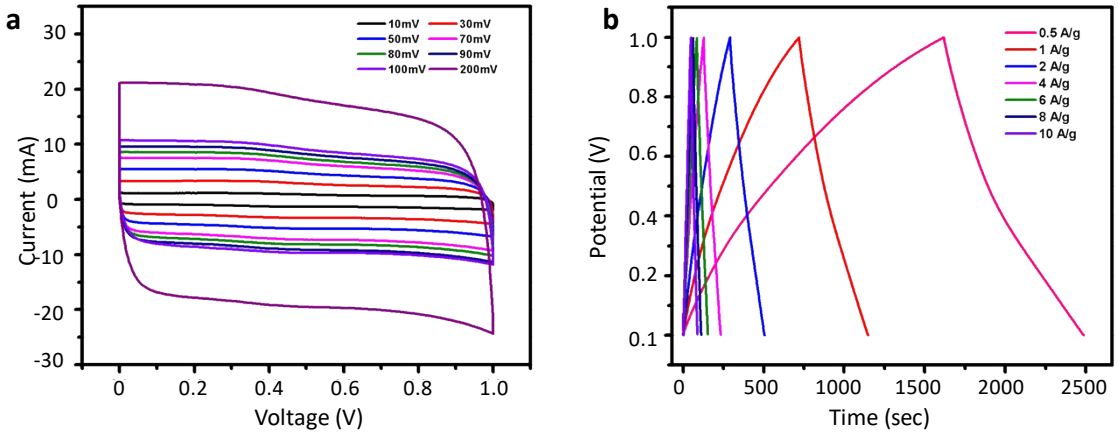

Figure S5. Electrochemical performance measured in 1 M H_2SO_4: (a) CV curves of 250-HADQ COF at different scan rates. (b) GCD curves of 250-HADQ COF at current densities between 0.5 A/g and 10 A/g.

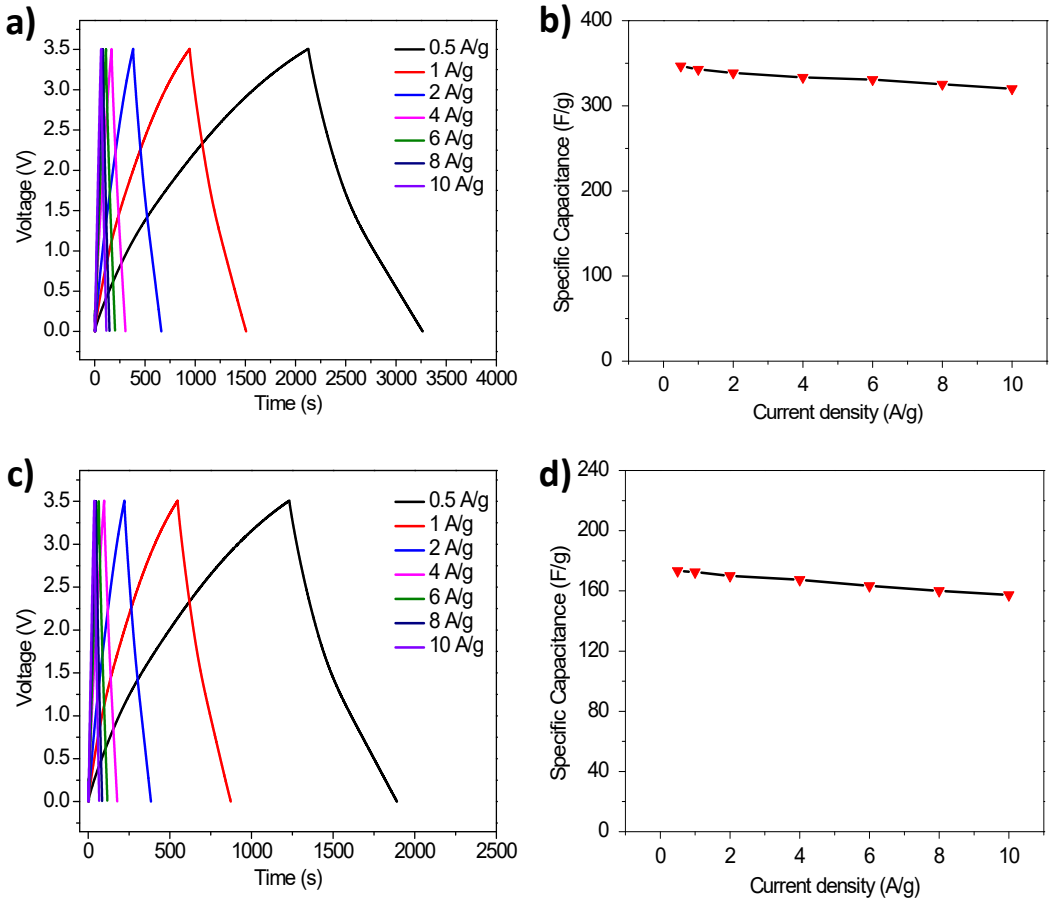

Figure S6. Electrochemical performance of 200-HADQ COF and pristine HADQ COF measured in ionic liquid ($EMIMBF_4$), respectively: (a, c) GCD curves at current densities between 0.5 A/g to 10 A/g. (b, d) Specific Capacitance at varying current densities.

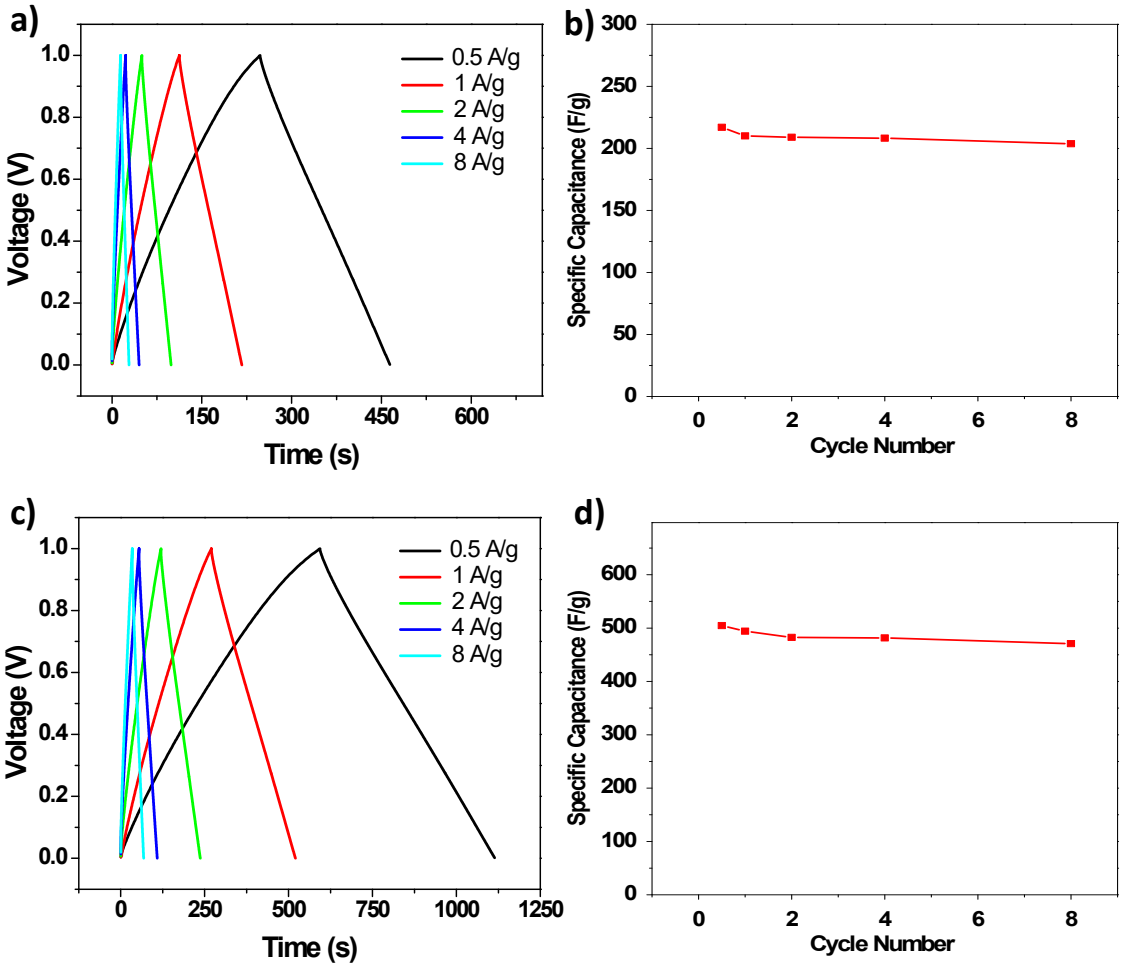

Figure S7. Electrochemical performance of pristine HADQ COF and 250-HADQ COF measured using three-electrode system in 1M H_2SO_4 respectively: (a, c) GCD curves at current densities between 0.5 A/g and 8 A/g. (b, d) Specific Capacitance at varying current densities.

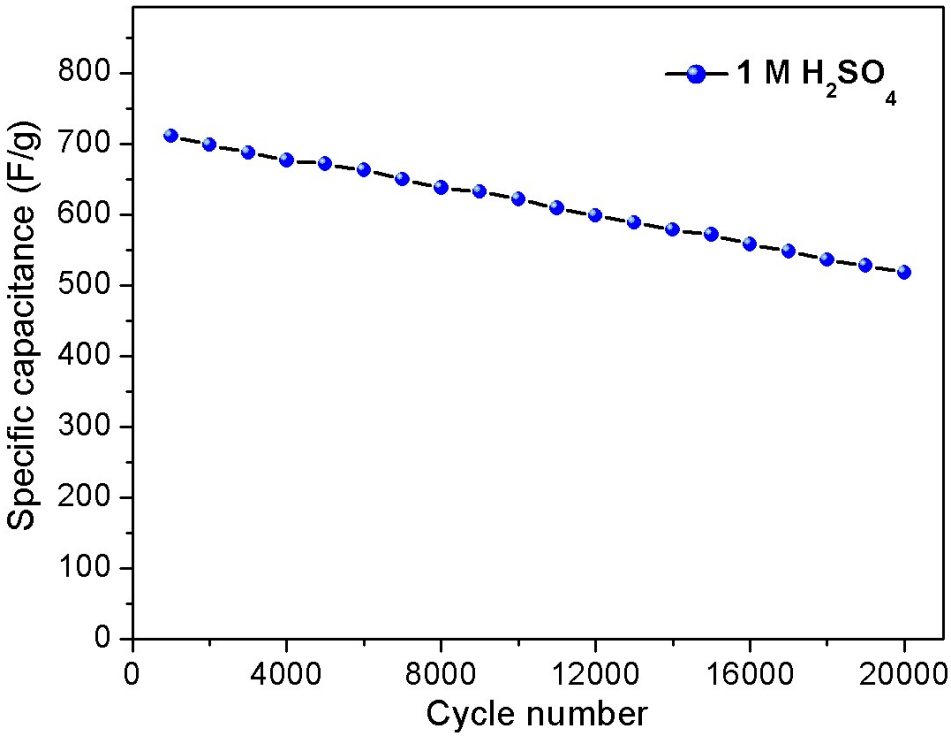

Figure S8. Cyclic performance of 250-HADQ COF in 1M H_2SO_4.

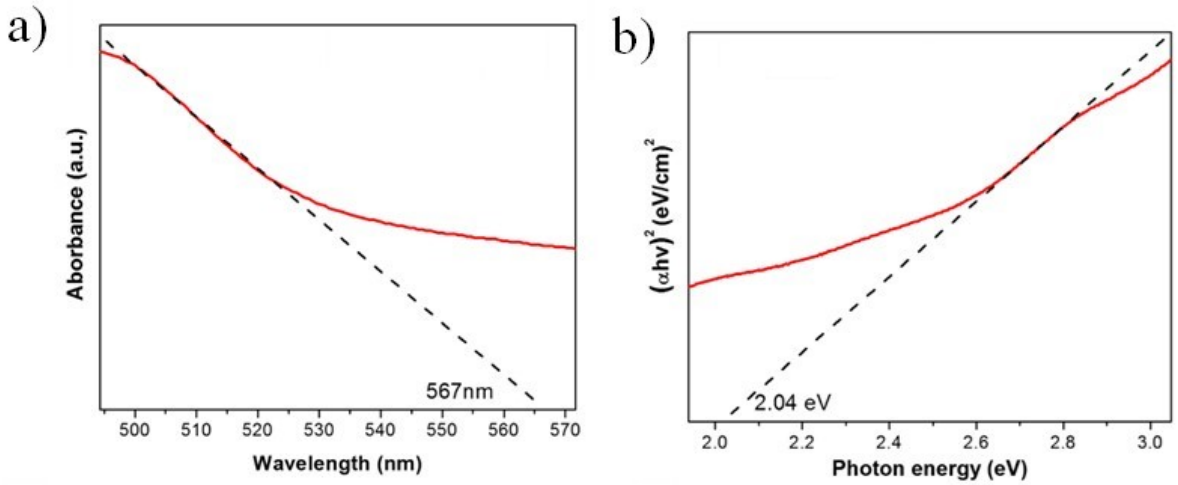

Figure S9. UV-VIS-NIR Spectrophotometer spectra of 250-HADQ COF, (b) Corresponding tauc plots of 250-HADQ COF.

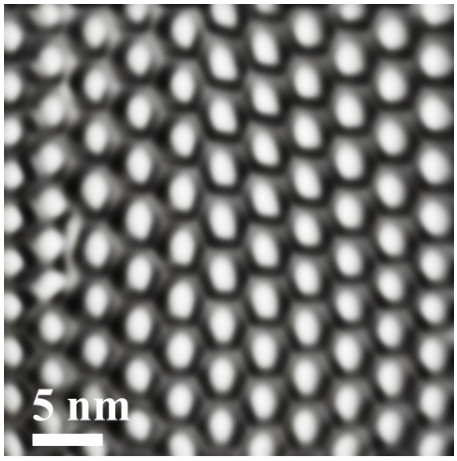

Figure S10. HRTEM image of Hexagonal pores of 250-HADQ COF.

Section 8. Energy/power density comparison with the reported double-layer supercapacitors

Table S2. Energy and power density comparison with reported double-layer supercapacitors

Electrode materials	**Electrolyte**	**Operation voltage (V)**	***Emax*** **(Wh/kg)**	***Pmax*** **(kW/kg)**	**Stability (cycles)**	**Ref.**
NiFe/rGO	1M KOH	1	-	-	89% (2000)	[1]
NGFs	PVA/H_3PO_4 gel electrolyte	2.4	19.5 μW h/cm^2 at	40 mW/cm^2 power density	95.8% (10,000)	[2]
GWAC	$EMIMBF_4$	3.5	80	70	98.8% (10000)	[1]
MEGO electrode	(BMIM BF_4)/AN	3.5	68	250	97% (10000)	[3]

HGP-based supercapacitors	(BMIM BF_4)/AN	3.5	77	338	90% (20000)	[4]
(CNFs@polypyrrole)	6M KOH	1.0	41.6	137	97% (3000)	[5]
Porous 3D graphene based bulk material	$EMIMBF_4$	3.5	98	100	94% (5000)	[6]
aG-O14 film electrode	$TEABF_4$/AN	2.8	26	100	95% (2000)	[7]
3DG1000-SC	$EMIMBF_4$	4	44	153	99%(20000)	[8]
3DG1000-SC	6 M KOH	1	8	10	91%(20000)	[8]
HGF-EC electrode	($EMIMBF_4$/AN)	3.5	74	2.5	94% (10000)	[9]
Triazine-Based Framework	$EMIMBF_4$	3.5	62.7	2	85% (10000)	[10]
flash-reduced graphene-oxide (FRGO)	$EMIMBF_4$	3.8	76	11	90% (1000)	[11]
LHC-3K	6M KOH	1	22.9	25,400	95% (5000)	[12]
PTPB-Z-900	$EMIMBF_4$	3.5	36	40,000	92%	[13]

					(10000)	
PBS-RGO-N	6M KOH	1	25	125	86% (10000)	[14]
AC//IL//MnO_2	$EMIMBF_4$	3	210	230	68% (5000)	[15]
250-HADQ COF	$EMIMBF_4$	3.5	219.4	87.5	89% (100,000)	This Work
250-HADQ COF	H_2SO_4	1	30.1	25	91% (10000)	

Section 9. Computational studies for molecular structure of HADQ COF

The DFTB approach with the LJ dispersion was used to investigate the molecular structure and electronic characteristics of monolayer and stacked HADQ COF isomers. The HOMO–LUMO energy gaps, as well as the associated LJ and crystal-stacking energies, were calculated. a=b=15.65 was the optimal lattice constant. Three distinct stacking configurations were adjusted using the optimized monomer: ideal AA, AA slip-stacked by 0.8 in the a and b directions, and AB. The lattice's third dimension, c, was set to 6.25, 6.25, and 5.25 for the AA, slipped AA, and AB structures, respectively. The slipping AA geometry is the HADQ COF's minimal energy structure. For each structure, HOMO–LUMO gaps have been determined and are displayed in Supplementary Table S1. The HOMO–LUMO gap of the HADQ COF monolayer is 0.65 eV, which is unaffected by any stacking configuration, while the HOMO–LUMO gaps of the slid AA, AA, and AB structures are 0.65, 0.68, and 0.62 eV, respectively.

$$a = b = 15.650861\ Å$$

c = 3.49006 Å

α = β = 90°

γ = 120°

Interlayer distance (D): 3.36 Å

Pawley refinement Rwp = 2.73%

Table S3. The total DFTB energies, LJ, and the total crystal stacking energies per monolayer as well as the corresponding HOMO LUMO energy gap for HADQ COF.

Stacking	*c* [Å]	Total DFTB Energy [a.u.]	LJ energy [a.u.]	Total crystal stacking energy [kcal mol–1]	HOMO-LUMO gap [eV]
Monolayer		-243.0177	1.162		0.6525
AA	6.07	-486.147851	2.2503	29.01	0.6575
Slipped AA (0.8 Å)	4.01	-486.406628	1.9768	110.20	0.6885
AB	4.49	-486.291736	2.1057	74.15	0.6213

Section 10. Computational setup for theoretical specific surface area of HADQ COF

The present study has been performed by using DFT with generalized gradient approximation (GGA) and the Perdew-Burke-Ernzerhof (PBE)[16] functional for the exchange-correlation potentials that have been accomplished through Vienna ab initio simulation package (VASP)[17-19]. In order to optimize the structure, a 5×5×1 k-points and 450 eV energy cutoff have been applied.

The COF was modeled via a periodic unit cell containing 30 atoms (18 carbon and 12 nitrogen atoms). The COF unit cell is hexagonal with unit-cell parameters a = b = 13.86, c = 3.94 Å and α = β = 90°; γ = 60° in reciprocal space and the periodic condition is employed along the a and b directions. The total energy was converged to an accuracy of 1×10^{-5} eV to obtain accurate forces, and a force tolerance of -0.02 eV/Å was applied in the structure optimization.

The theoretical surface area of COF materials is calculated as;

One proton mass is $m_p = 1.6726231 \times 10^{-27}$ kg;

one C atom mass: $12 \times m_p = 12 \times 1.6726231 \times 10^{-27} = 2.00714772 \times 10^{-26}$ kg;

one N atom mass: $14 \times m_p = 14 \times 1.6726231 \times 10^{-27} = 2.34167234 \times 10^{-26}$ kg

Total mass:

$M = 18\ C + 12\ N = 18 \times 2.00714772 \times 10^{-26} + 12 \times 2.34167234 \times 10^{-26} = 64.22872704 \times 10^{-24}$ kg

per area;

$A = a \times b \times \sin 60\ (Å^2) = 13.86 \times 13.86 \times \sin 60^\circ = 166.3631337\ (Å^2)$

$$A/M = \frac{166.3631337\ Å^2}{64.22872704 \times 10^{-26}\ Kg} = 2.59016707 \times 10^{26}\ Å^2/\text{kg}$$

$A/M = 2590.1670689071\ (m^2/g)$

Therefore, the theoretical surface is of COF materials is 2590.1670689071 (m^2/g) which is consistent with experimental measured BET surface area of COF (2743 m^2/g).

Table S4. Fractional atomic coordinates of AA stacked structure for 250-HADQ COF.

Atom	x	y	z	population
H	-2.26072953	4.60735469	4.17854197	0.9122687
H	4.46614391	4.54094576	4.17974516	0.91319645
H	4.42140739	0.18259102	4.09171623	0.9134171
H	-2.31222895	0.24661488	4.14964901	0.90963096
H	-1.49092432	-3.57807145	4.19959604	0.90799854
H	3.51558444	-3.63445859	4.27276397	0.91299108
H	-1.40220622	8.37561207	4.34461959	0.90747193
H	3.60340717	8.39288914	4.37520873	0.90726421
H	-2.45219629	-5.21779861	4.43230721	0.90798127
H	0.03677724	-9.54330152	4.02761189	0.90692375
H	4.42183807	-5.28756186	4.65370267	0.91138829
H	1.87005292	-9.57030663	4.1865389	0.90596618
H	-2.3422249	9.99423884	4.28676009	0.90670395
H	0.11690421	14.30403276	4.94149312	0.91146701
H	4.52992152	10.04136906	4.25753754	0.90792347
H	2.0133882	14.32968688	4.82125479	0.91323713
H	8.25830917	11.23465776	4.07764722	0.90904984
H	12.00492877	13.45945976	3.89984499	0.91114568
H	-6.17372919	-6.41600626	4.44039499	0.91250839
H	-9.93474838	-8.60140616	4.50894276	0.91158402
H	-6.1214765	11.15902838	4.11700589	0.90977986
H	-9.87856982	13.36302336	4.09756457	0.90853632
H	8.08627355	-6.51448048	4.5944103	0.90911573
H	11.85875236	-8.69635486	4.68964753	0.91346704
H	6.55592268	0.37201326	4.92854617	0.93351878
H	6.50309296	0.41257481	3.14912801	0.93371103
H	7.9167471	1.02282427	4.01420375	0.93761137
H	6.34202746	4.20371916	2.83346363	0.93260486

H	7.7649435	3.15837219	2.7428746	0.9376714
H	6.2672325	2.68925885	1.91397561	0.93327209

H	7.83920765	3.11961841	5.37272909	0.93742556
H	6.40701634	4.15595414	5.40797025	0.93319912
H	6.39886378	2.60951495	6.27278915	0.93332067
H	-4.45181058	0.53112686	3.27154955	0.93307815
H	-4.38857618	0.51104526	5.05157529	0.93020021
H	-5.79397314	1.18402468	4.21772983	0.93992536
H	-4.16064073	4.30761189	5.44824084	0.9340754
H	-5.59315696	3.27365651	5.5385753	0.93975189
H	-4.09108064	2.78505582	6.35046649	0.92779602
H	-5.62805066	3.28939783	2.86137841	0.93920668
H	-4.17500845	4.29752966	2.88317187	0.93254219
H	-4.17009667	2.76417722	1.99276352	0.93052493
H	-9.39611778	11.7382855	1.79029868	0.93306369
H	-7.86449175	10.82804143	1.75474033	0.93140689
H	-9.41941871	9.95672786	1.7588134	0.93144979
H	-7.89015967	9.47904494	5.15711802	0.92361163
H	-8.76467448	8.6227865	3.88271482	0.9393723
H	-7.20165067	9.35608016	3.53405385	0.93542722
H	-10.78681085	9.7869975	3.91919589	0.93936701
H	-10.43093	10.917771	5.22521259	0.92227279
H	-10.94886747	11.52178643	3.6471814	0.93423656
H	9.66326463	9.54335804	4.87977719	0.929429
H	9.44214986	9.54825051	3.1129732	0.93289623
H	10.80629759	8.69177222	3.83503731	0.94117346
H	12.43021085	11.72510231	2.29544738	0.93224787
H	12.35203536	9.95555876	2.27835517	0.94046568
H	11.00971776	10.91152797	1.62398032	0.92601237
H	12.6334709	9.8358804	4.97143331	0.940771
H	12.94762272	11.56018782	4.74854276	0.93549786
H	11.71693202	11.04215185	5.9250925	0.92101065
H	12.44090708	-6.95362384	3.22068113	0.93354438
H	11.07060218	-6.22988969	2.35832589	0.93244897

H	12.29600906	-5.19289891	3.11597148	0.93655943

H	9.35265453	-4.76836518	5.41298783	0.93354742
H	10.56776402	-3.93568391	4.43864848	0.93728726
H	9.29846422	-4.86175763	3.63487921	0.93319728
H	12.38086539	-5.0288736	5.75027429	0.93688409
H	11.24477687	-6.00062372	6.70786991	0.93268497
H	12.56032772	-6.78789199	5.81616143	0.93386333
H	-8.75414492	-5.64104561	6.59338865	0.93305391
H	-7.41657368	-4.91120051	5.68447747	0.93345483
H	-9.01231795	-4.14967282	5.66578167	0.93751985
H	-8.7215941	-5.83949254	2.2390938	0.93256623
H	-9.02249711	-4.27297239	3.01911706	0.93767575
H	-7.4135683	-5.0014175	3.09641573	0.93306417
H	-10.91673506	-5.11510482	4.36648624	0.93735076
H	-10.80359088	-6.67728061	3.55536764	0.93384304
H	-10.82156953	-6.58603864	5.33149503	0.93362146
H	-3.67351227	1.14530453	-0.10285151	0.91340778
H	3.0598639	1.08635544	-0.16905363	0.90958074
H	3.01314011	-3.27453847	-0.15044679	0.91219713
H	-3.71412521	-3.2135702	-0.16354055	0.91320312
H	-2.84834524	-7.05952835	-0.27138055	0.90705854
H	2.15743555	-7.04342903	-0.2193385	0.90740725
H	-2.76617967	4.96728863	-0.23114709	0.91300843
H	2.24091764	4.89640071	-0.17131621	0.9076866
H	-3.77075793	-8.69484719	-0.08319663	0.9072009
H	-1.27494056	-12.99314251	-0.6619685	0.91282813
H	3.09899504	-8.65915306	-0.18907857	0.90668898
H	0.63443642	-12.96995157	-0.81605513	0.91141037
H	-3.66122386	6.62783245	-0.63091266	0.9114237
H	-1.10278116	10.89724355	-0.08305699	0.90634853
H	3.20221787	6.52325031	-0.37917948	0.90769446
H	0.74151346	10.8531986	0.14202357	0.90710215
H	6.98848628	7.73405022	-0.4141573	0.91293124

H	10.71246678	9.98377959	-0.55494922	0.91165206

H	-7.59772261	-9.89471748	0.06343654	0.91205594
H	-11.27604762	-12.2315506	0.19915973	0.9076601
H	-7.33042641	7.85733825	-0.60281357	0.91180691
H	-11.09571643	10.05235886	-0.68214402	0.91090072
H	6.89029403	-9.8124778	-0.12133101	0.90985316
H	10.64519466	-12.01974607	-0.09582989	0.90853734
H	4.91355634	-1.42530686	2.01382926	0.93050393
H	4.92845395	-2.96016297	1.12623544	0.93248386
H	6.37710028	-1.94603332	1.15200518	0.93921201
H	4.84923537	-1.45465674	-2.3439213	0.92790604
H	6.34816615	-1.94272872	-1.52593776	0.93968066
H	4.91441369	-2.97537696	-1.43811169	0.93407872
H	6.54340628	0.15301521	-0.20843761	0.93990808
H	5.14073138	0.82146938	-1.05045565	0.93082499
H	5.19601012	0.80674293	0.72986497	0.9330378
H	-5.65527609	-1.28324323	-2.26948047	0.93334166
H	-5.65826962	-2.82958632	-1.40424047	0.93322286
H	-7.09214569	-1.79553487	-1.36513065	0.9374402
H	-5.51102282	-1.36131714	2.08895985	0.93324789
H	-7.01238695	-1.828524	1.26556619	0.93769695
H	-5.5916007	-2.87616564	1.17064566	0.93265567
H	-7.16727793	0.30401799	-0.00706907	0.93761876
H	-5.75041977	0.91560274	0.85187614	0.93369997
H	-5.80997557	0.95381008	-0.92737987	0.93354989
H	-9.95043786	6.97862636	-2.66906556	0.932916
H	-8.59039119	6.30553277	-1.75104448	0.93366096
H	-10.18046256	5.53626705	-1.66031791	0.93688253
H	-9.8378734	7.39595131	1.66902287	0.93230545
H	-10.15703443	5.79355717	0.97318859	0.93684849
H	-8.54849929	6.51475332	0.82951789	0.93325115
H	-12.08047275	6.5865843	-0.41590924	0.93704449
H	-11.9390064	8.17235166	0.34792205	0.93328763

H	-11.97079924	8.03038838	-1.42802945	0.93361377

H	9.81340886	7.1789579	1.64543739	0.93285157
H	8.4174344	6.34412969	0.93665406	0.93342898
H	10.03006417	5.62709761	0.80954253	0.9373896
H	9.32859259	7.02503008	-2.68534717	0.93241375
H	9.75991094	5.54017808	-1.81565751	0.93747998
H	8.14416744	6.23107897	-1.63120571	0.93362507
H	11.76188423	6.55976959	-0.76162069	0.93750278
H	11.49488531	8.06318243	-1.64842163	0.93273584
H	11.69467905	8.0869086	0.12162859	0.93386644
H	8.65181697	-8.14089801	-1.15975077	0.92366207
H	7.97724289	-8.00126971	0.4675123	0.93532362
H	9.54187853	-7.27894735	0.09943975	0.93937646
H	10.15668826	-10.39792671	2.20843826	0.93329538
H	10.15766379	-8.61666145	2.2495184	0.93108672
H	8.61411807	-9.50658354	2.23509757	0.93135121
H	11.56359279	-8.45261606	0.13866026	0.93980394
H	11.70957361	-10.19905725	0.33241499	0.93405922
H	11.20678645	-9.51819826	-1.21985494	0.92229065
H	-10.36871523	-9.87702061	2.53158622	0.92315117
H	-9.04114806	-8.85002006	1.92042192	0.9304191
H	-10.68905519	-8.20206543	2.02838883	0.94092922
H	-10.3392755	-8.76537342	-1.63331323	0.92663797
H	-10.50654833	-7.5395471	-0.36732058	0.94165397
H	-8.93222213	-8.28988559	-0.65395254	0.93137687
H	-12.4646021	-8.90869171	0.33235328	0.93948591
H	-12.17291133	-10.279868	-0.74517428	0.93261935
H	-12.29401596	-10.52317257	1.01679555	0.93277793
C	4.66124324	2.35997072	4.12860284	3.993732
C	3.94276623	3.57118554	4.16605327	4.09356803
C	2.53708781	3.60406859	4.17802109	4.00771259
C	1.80219864	2.3858348	4.16158755	4.00313815
C	2.51507381	1.15728191	4.1439241	4.00723276

C	3.92342429	1.1632579	4.12015252	4.09648899

C	1.82243091	4.88224614	4.20739931	3.85641772
C	0.35371297	2.39644368	4.16079501	4.00745872
C	-0.35748082	3.62522919	4.16876777	4.00843271
C	-1.76195934	3.62495789	4.16682005	4.08874555
C	-2.50512017	2.4300249	4.15931464	3.98436893
C	-1.79433725	1.21750574	4.15140807	4.09120735
C	-0.38591893	1.18404331	4.15238108	4.01104418
C	1.77553776	-0.10656938	4.15848894	3.85387109
C	0.32849773	-0.09237253	4.1609742	3.85630754
C	0.30940503	-2.39648916	4.21034343	3.85354049
C	1.74404435	-2.41125407	4.22029609	3.85118806
C	-0.3931473	-3.62985322	4.23140471	4.13564077
C	2.41606505	-3.66047548	4.27326296	4.13529394
C	1.71904527	-4.87235089	4.31829137	3.978439
C	0.37697544	4.88815495	4.19639282	3.85485659
C	0.38705559	7.1879305	4.27075145	3.85277874
C	1.82130674	7.18704016	4.28266095	3.85272702
C	-0.30430985	8.42366997	4.33262166	4.13511504
C	2.50501385	8.42969165	4.34938554	4.1342327
C	1.81892264	9.64767665	4.40689693	3.98228361
C	0.27427232	-4.85729537	4.28309589	3.97937565
C	-0.47402521	-6.12495972	4.27540256	3.98121945
C	-1.87137848	-6.14581246	4.33242237	4.13344989
C	0.24109006	-7.37593983	4.19660478	3.98182624
C	2.43840081	-6.15551364	4.3780224	3.98029694
C	-2.60040123	-7.3638601	4.28850882	3.8539121
C	-0.47192187	-8.57336328	4.10762927	4.13590503
C	1.70675858	-7.39439071	4.26466362	3.98172682
C	3.8270562	-6.2050109	4.53306472	4.14029407
C	-1.88616365	-8.59998578	4.15285002	3.85294694
C	2.39682035	-8.60975378	4.26852362	4.1367185
C	4.53388934	-7.43688801	4.52760804	3.85541606

C	3.80767496	-8.66577258	4.38251713	3.85311858

C	0.37436298	9.64314145	4.4030986	3.98257651
C	-0.3702091	10.90797979	4.4952174	3.98325433
C	-1.76826631	10.92092149	4.42843095	4.13394961
C	0.34584843	12.15179096	4.66149733	3.98363425
C	2.54750889	10.92538974	4.47738022	3.97843181
C	-2.51334431	12.1244114	4.52655047	3.84932298
C	-0.38545246	13.33641554	4.79704234	4.14028062
C	1.81956902	12.16390565	4.63395536	3.9803185
C	3.94300183	10.96160573	4.38703577	4.13348474
C	-1.80364142	13.35539033	4.72307896	3.85438982
C	2.53199579	13.36714193	4.70356863	4.13878668
C	4.6678933	12.18117518	4.43986972	3.85121438
C	3.9478069	13.41108945	4.59927412	3.85194331
C	6.65753093	13.34681561	4.3661181	3.85319502
C	-4.58512842	-8.5314128	4.33371146	3.85730823
C	6.50323911	-8.62595534	4.58665301	3.85993738
C	-4.51905045	13.26453602	4.51125861	3.85310913
C	5.93095677	14.59076691	4.50541808	3.8534672
C	-3.79926753	14.50731108	4.69010467	3.85892511
C	-3.86264877	-9.77429553	4.19740994	3.8542244
C	5.77234009	-9.86539139	4.45241904	3.85208495
C	8.11628455	13.36565136	4.24460289	4.01196943
C	8.80178476	14.60931893	4.27838851	4.00734344
C	8.84180286	12.1675988	4.09216701	4.09399996
C	10.2163706	14.6119841	4.14926971	4.00790739
C	10.24282189	12.16050548	3.96908811	3.98297739
C	10.90900358	13.40018561	3.99531887	4.08817929
C	-6.04375731	-8.55409603	4.41518858	4.00985644
C	-6.76185519	-7.34786865	4.45547061	4.09410608
C	-6.73170422	-9.79836495	4.41911954	4.00356037
C	-8.16835514	-7.32296769	4.47424194	3.99580652
C	-8.14836426	-9.79046525	4.50489095	4.01210738

C	-8.835937	-8.55897162	4.50745312	4.09484293

C	-5.98161746	13.28070178	4.4086605	4.00782581
C	-6.70314725	12.08970786	4.2003953	4.09409507
C	-6.67736598	14.51681562	4.50891324	4.00939167
C	-8.10779236	12.07811083	4.09628421	3.9832134
C	-8.0949674	14.52043312	4.39185283	4.00823537
C	-8.78293429	13.30936898	4.19132353	4.09431821
C	7.96076068	-8.64907661	4.64636341	4.01131257
C	8.68141463	-7.4389249	4.63063741	4.09689523
C	8.64455237	-9.89388111	4.6615822	4.00503409
C	10.08610921	-7.41429977	4.64018374	3.99385741
C	10.06472457	-9.8200255	4.71750481	4.00720987
C	10.75732635	-8.65155162	4.70115587	4.09329836
C	6.20771926	2.38809509	4.0913485	3.89288989
C	6.81750278	0.97148136	4.04393482	4.22016257
C	6.66716782	3.15289959	2.82747223	4.21595776
C	6.7383917	3.1082589	5.35390384	4.21651849
C	-4.04741197	2.50294058	4.17219063	3.89227527
C	-4.69616229	1.1051815	4.17829775	4.22068804
C	-4.4961816	3.25956896	5.44515147	4.21788814
C	-4.52837123	3.25598707	2.90940595	4.21687648
C	-8.86342513	10.79847046	3.67734696	3.89204135
C	-8.88752429	10.83400302	2.15380922	4.2185204
C	-8.1386752	9.50329605	4.09140463	4.22942076
C	-10.33123961	10.76226869	4.14840857	4.22913534
C	11.06973241	10.86514776	3.81283547	3.89119075
C	10.19201837	9.60216501	3.91728894	4.22168939
C	11.75399843	10.86775625	2.42862847	4.21910842
C	12.1489068	10.82290872	4.92046954	4.22681034
C	10.88781265	-6.09837725	4.54381038	3.89260407
C	11.72017506	-6.1227948	3.24013309	4.21610616
C	9.97058807	-4.85795969	4.50657742	4.21909748
C	11.81974135	-5.97584192	5.77038265	4.2158231

C	-8.90216705	-5.96225807	4.42494853	3.89189914

C	-8.49614311	-5.12212438	5.65839749	4.21594678
C	-8.48921754	-5.23024506	3.12537757	4.21628489
C	-10.43810855	-6.10493032	4.42086365	4.22050643
C	3.25611228	-1.09688308	-0.15668262	3.98427029
C	2.54369338	0.11458662	-0.16096681	4.09127544
C	1.13522435	0.1457036	-0.16007167	4.01090698
C	0.39630434	-1.06624985	-0.15683665	4.00758746
C	1.10944889	-2.29338581	-0.15043697	4.00831876
C	2.51391959	-2.29230992	-0.15017986	4.08880451
C	0.41888254	1.420055	-0.16764943	3.85634887
C	-1.05221418	-1.05579125	-0.15799012	4.00318737
C	-1.76673925	0.17160463	-0.14860227	4.00719141
C	-3.1750243	0.16477082	-0.1260877	4.09661137
C	-3.91194949	-1.03244655	-0.12817067	3.99370591
C	-3.19208797	-2.24301443	-0.15642332	4.09361949
C	-1.78629767	-2.27393065	-0.16455296	4.00754026
C	0.37580106	-3.55606557	-0.15485979	3.85491911
C	-1.06951431	-3.55048175	-0.17127839	3.8565434
C	-1.06634202	-5.85440591	-0.1966065	3.85274658
C	0.36764919	-5.8555442	-0.1764962	3.85273002
C	-1.7503029	-7.09673573	-0.23961095	4.13434767
C	1.05956051	-7.09167977	-0.21229294	4.13505178
C	0.38072134	-8.31145067	-0.2699182	3.98246093
C	-1.02802479	1.43518857	-0.16148499	3.85384765
C	-0.9965426	3.7395056	-0.20116515	3.85114792
C	0.43795127	3.72223148	-0.19641741	3.85364085
C	-1.66656568	4.99047092	-0.23522045	4.13528449
C	1.1435049	4.95258628	-0.20079078	4.13571578
C	0.47826681	6.18094472	-0.23073375	3.97954384
C	-1.06392095	-8.31468516	-0.27194697	3.98238621
C	-1.79584703	-9.5901154	-0.32340875	3.97813411
C	-3.19176912	-9.61884382	-0.22094793	4.13394792

C	-1.06779476	-10.82844966	-0.47995408	3.97987193

C	1.12529262	-9.57593769	-0.36516245	3.98315102
C	-3.92562055	-10.83270909	-0.2795354	3.85112189
C	-1.78685136	-12.02678023	-0.54600993	4.13791744
C	0.40687434	-10.81952366	-0.52333312	3.98348593
C	2.52458304	-9.58652745	-0.32432734	4.13413238
C	-3.20364472	-12.05978821	-0.44792337	3.85231089
C	1.13860296	-12.00223487	-0.67712561	4.13982305
C	3.27123024	-10.78689284	-0.44825366	3.84945202
C	2.55948324	-12.01813867	-0.63755238	3.85423351
C	-0.96624821	6.20088	-0.26489218	3.9783959
C	-1.68077157	7.48715666	-0.3138249	3.98038524
C	-3.06654214	7.54260586	-0.4907317	4.14024542
C	-0.9463683	8.72182803	-0.17446481	3.98182271
C	1.23220365	7.44331525	-0.19784107	3.98106218
C	-3.76983218	8.77656303	-0.48913389	3.85559567
C	-1.63332974	9.93986785	-0.18053915	4.13620925
C	0.51958132	8.69373124	-0.08993044	3.98146213
C	2.63029549	7.4538307	-0.25578344	4.13390603
C	-3.04260043	10.00248895	-0.32375026	3.85317892
C	1.24182009	9.88144002	0.03334529	4.1354504
C	3.3702191	8.66392987	-0.18870337	3.85398267
C	2.65658045	9.89680596	-0.02111881	3.85245434
C	5.36007134	9.82619593	-0.23046721	3.85724093
C	-5.92212083	-11.99510299	-0.22675052	3.85206074
C	5.28230693	-11.91979771	-0.49073085	3.8529725
C	-5.73659548	9.96965906	-0.58025395	3.85939882
C	4.63455336	11.06313944	-0.07569655	3.85512721
C	-5.00500812	11.20740603	-0.43437875	3.8516836
C	-5.18944724	-13.23576752	-0.37965542	3.85505501
C	4.5616537	-13.16263602	-0.66602183	3.85927477
C	6.81929373	9.86949	-0.32626376	4.00875394
C	7.4938179	11.12344962	-0.30810995	4.0037868

C	7.55773881	8.67754903	-0.41767952	4.09496801

C	8.9085164	11.1366542	-0.4097404	4.01008996
C	8.96332637	8.67709134	-0.49314691	3.993265
C	9.6162598	9.92137137	-0.49408024	4.09906815
C	-7.38561991	-12.02837678	-0.11861989	4.01182087
C	-8.146786	-10.84969282	0.02956005	4.09086519
C	-8.04661302	-13.28908198	-0.15636315	4.00714115
C	-9.55464172	-10.87606066	0.13622201	3.98252978
C	-9.45815396	-13.31917679	-0.03465339	4.00731368
C	-10.18489703	-12.12815484	0.108382	4.09254948
C	-7.19442524	9.99472486	-0.65192606	4.01139662
C	-7.91801307	8.78869129	-0.63784836	4.09458722
C	-7.87977536	11.24032204	-0.66311802	4.00512997
C	-9.32604344	8.76425244	-0.63889476	3.9938017
C	-9.29958558	11.22662682	-0.71443044	4.00739158
C	-9.99632508	9.99810972	-0.69714876	4.09491504
C	6.7470197	-11.9349794	-0.4077598	4.00786747
C	7.47058182	-10.74402875	-0.20503676	4.09404424
C	7.44337835	-13.17136502	-0.50871158	4.00924494
C	8.87561263	-10.73324619	-0.10338156	3.98332846
C	8.86152721	-13.1770824	-0.38818593	4.0083879
C	9.54976763	-11.96562931	-0.19193511	4.09425806
C	4.79843471	-1.16814914	-0.16640108	3.89227061
C	5.27751816	-1.91720323	1.09950293	4.21695639
C	5.25087448	-1.92761942	-1.4362646	4.21775163
C	5.44532389	0.23039073	-0.17407812	4.22070734
C	-5.45830588	-1.06115536	-0.08863052	3.89288058
C	-5.99127252	-1.78243684	-1.34950432	4.21641579
C	-5.91492451	-1.82477692	1.17710134	4.21596756
C	-6.06816449	0.3554524	-0.04099483	4.22014614
C	-10.05751522	7.41033438	-0.51806223	3.89256435
C	-9.67067233	6.51048326	-1.71391253	4.21602098
C	-9.62460383	6.74286081	0.80949466	4.21635735

C	-11.59093649	7.56874937	-0.50402058	4.21889087

C	9.72704632	7.33455991	-0.54483891	3.89267422
C	9.48092203	6.58101276	0.78370098	4.21546778
C	9.20883767	6.48954468	-1.73240109	4.2168885
C	11.24721639	7.53195354	-0.71727874	4.21966876
C	9.62989549	-9.45438752	0.32138957	3.89191564
C	8.90903102	-8.15777668	-0.09599586	4.22939688
C	9.64064768	-9.49776731	1.84508318	4.21873893
C	11.10121766	-9.41262752	-0.13745308	4.22904624
C	-10.38972132	-9.59653081	0.37005958	3.8915819
C	-10.10379462	-9.10492421	1.79455074	4.22101965
C	-10.01304305	-8.48986864	-0.62359003	4.2217117
C	-11.90711099	-9.85304004	0.23413537	4.21962389
N	-0.37841887	-1.22307142	4.1793971	5.27540086
N	-0.31652288	6.02535763	4.22389066	5.27481324
N	2.45769799	-1.25241218	4.18476904	5.2783554
N	2.52056639	6.01863578	4.24763988	5.2778633
N	6.02478307	12.17305696	4.3326886	5.27565608
N	4.60107709	14.60669625	4.62273696	5.28174082
N	-3.87213113	12.10123611	4.42969006	5.27081029
N	-2.47059068	14.53877068	4.79956413	5.28217582
N	-3.95836085	-7.35437864	4.37346573	5.27995564
N	-2.53419213	-9.79455441	4.10317811	5.27426195
N	4.44291586	-9.8693672	4.35375423	5.26961087
N	5.88935517	-7.44299534	4.63151833	5.28018515
N	-1.76720546	-4.68711311	-0.19007709	5.27776131
N	-1.71069414	2.58093521	-0.17649147	5.27843352
N	1.07073617	-4.69247259	-0.15251242	5.27472929
N	1.12635478	2.54968152	-0.1200587	5.27531341
N	4.72929516	8.65077373	-0.28258237	5.27959379
N	3.30798884	11.08659195	0.03841658	5.27428172
N	-5.12361703	8.78610625	-0.61680388	5.28029981
N	-3.67731869	11.20744401	-0.30768465	5.26990515

N	-5.28509966	-10.82353641	-0.17787169	5.27553938

N	-3.86020778	-13.25121939	-0.49392009	5.27881112
N	3.23007462	-13.19742709	-0.74264384	5.28211881
N	4.63226553	-10.7599792	-0.38347221	5.27058974

Section 11. References

[1] C. Li, X. Zhang, Z. Lv, K. Wang, X. Sun, X. Chen, Y. Ma, Scalable combustion synthesis of graphene-welded activated carbon for high-performance supercapacitors, Chemical Engineering Journal, 414 (2021) 128781.

[2] K. Kang, Z. Wu, M. Zhao, Z. Li, Y. Ma, J. Zhang, Y. Wang, M. Sajjad, R. Tao, L. Qiu, A nanostructured covalent organic framework with readily accessible triphenylstibine moieties for high-performance supercapacitors, Chemical Communications, 58 (2022) 3649-3652.

[3] Y. Zhu, S. Murali, M.D. Stoller, K.J. Ganesh, W. Cai, P.J. Ferreira, A. Pirkle, R.M. Wallace, K.A. Cychosz, M. Thommes, D. Su, E.A. Stach, R.S. Ruoff, Carbon-Based Supercapacitors Produced by Activation of Graphene, Science, 332 (2011) 1537-1541.

[4] Y. Xu, C.Y. Chen, Z. Zhao, Z. Lin, C. Lee, X. Xu, C. Wang, Y. Huang, M.I. Shakir, X. Duan, Solution Processable Holey Graphene Oxide and Its Derived Macrostructures for High-Performance Supercapacitors, Nano Lett, 15 (2015) 4605-4610.

[5] L.-F. Chen, X.-D. Zhang, H.-W. Liang, M. Kong, Q.-F. Guan, P. Chen, Z.-Y. Wu, S.-H. Yu, Synthesis of Nitrogen-Doped Porous Carbon Nanofibers as an Efficient Electrode Material for Supercapacitors, ACS Nano, 6 (2012) 7092-7102.

[6] L. Zhang, F. Zhang, X. Yang, G. Long, Y. Wu, T. Zhang, K. Leng, Y. Huang, Y. Ma, A. Yu, Y. Chen, Porous 3D graphene-based bulk materials with exceptional high surface area and excellent conductivity for supercapacitors, Sci Rep, 3 (2013) 1408.

[7] L.L. Zhang, X. Zhao, M.D. Stoller, Y. Zhu, H. Ji, S. Murali, Y. Wu, S. Perales, B. Clevenger, R.S. Ruoff, Highly conductive and porous activated reduced graphene oxide films for high-power supercapacitors, Nano Lett, 12 (2012) 1806-1812.

[8] J. Zhao, Y. Jiang, H. Fan, M. Liu, O. Zhuo, X. Wang, Q. Wu, L. Yang, Y. Ma, Z. Hu, Porous 3D Few-Layer Graphene-like Carbon for Ultrahigh-Power Supercapacitors with Well-Defined Structure-Performance Relationship, Adv Mater, 29 (2017).

[9] Y. Xu, Z. Lin, X. Zhong, X. Huang, N.O. Weiss, Y. Huang, X. Duan, Holey graphene frameworks for highly efficient capacitive energy storage, Nat Commun, 5 (2014) 4554.

[10] L. Hao, J. Ning, B. Luo, B. Wang, Y. Zhang, Z. Tang, J. Yang, A. Thomas, L. Zhi, Structural evolution of 2D microporous covalent triazine-based framework toward the study of high-performance supercapacitors, J Am Chem Soc, 137 (2015) 219-225.
[11] S.I. Wong, H. Lin, J. Sunarso, B.T. Wong, B. Jia, Optimization of ionic-liquid based electrolyte concentration for high-energy density graphene supercapacitors, Applied Materials Today, 18 (2020) 100522.
[12] N. Guo, M. Li, X. Sun, F. Wang, R. Yang, Enzymatic hydrolysis lignin derived hierarchical porous carbon for supercapacitors in ionic liquids with high power and energy densities, Green Chemistry, 19 (2017) 2595-2602.
[13] J. Liang, Z. Xiao, Y. Gao, X. Xu, D. Kong, M. Wagner, L. Zhi, Ionothermal strategy towards template-free hierarchical porous carbons for supercapacitive energy storage, Carbon, 143 (2019) 487-493.
[14] Y. Chang, L. Zhou, Z. Xiao, J. Liang, D. Kong, Z. Li, X. Zhang, X. Li, L. Zhi, Embedding Reduced Graphene Oxide in Bacterial Cellulose-Derived Carbon Nanofibril Networks for Supercapacitors, ChemElectroChem, 4 (2017) 2448-2452.
[15] S. Maiti, A. Pramanik, S. Mahanty, Influence of imidazolium-based ionic liquid electrolytes on the performance of nano-structured MnO 2 hollow spheres as electrochemical supercapacitor, Rsc Advances, 5 (2015) 41617-41626.
[16] J.P. Perdew, A. Ruzsinszky, G.I. Csonka, O.A. Vydrov, G.E. Scuseria, L.A. Constantin, X. Zhou, K. Burke, Restoring the Density-Gradient Expansion for Exchange in Solids and Surfaces, Physical Review Letters, 100 (2008) 136406.
[17] G. Kresse, J. Furthmüller, Efficiency of ab-initio total energy calculations for metals and semiconductors using a plane-wave basis set, Computational Materials Science, 6 (1996) 15-50.
[18] G. Kresse, J. Furthmüller, Efficient iterative schemes for total-energy calculations using a plane-wave basis set, Physical Review B, 54 (1996) 11169-11186.
[19] G. Kresse, J. Hafner, Ab initio molecular dynamics for liquid metals, Physical Review B, 47 (1993) 558-561.